Heliyon 9 (2023) e21744

Contents lists available at ScienceDirect

Heliyon

journal homepage: www.cell.com/heliyon

Exploring the mechanism of Liuwei Dihuang formula for promoting melanin synthesis in juvenile zebrafish based on network pharmacology and molecular docking

Dandan Wang [a], Yan Yang [b], Gulijiayina Hengerjia [b], Yan Deng [c,*]

[a] Clinical Pharmacy Center, Nanfang Hospital, Southern Medical University, Guangzhou, 510515, China
[b] School of Pharmaceutical Sciences, Southern Medical University, Guangzhou, 510515, China
[c] School of Traditional Chinese Medicine, Southern Medicial University, Guangzho, 510515, China

ARTICLE INFO

Keywords:
LDF
Vitiligo
Network pharmacology
Oxidative stress factors
Nrf2/HO-1 pathway

ABSTRACT

Background: Vitiligo stands as a challenging skin disorder with limited treatment options available. LiuWei DiHuang formula (LDF), a renowned Traditional Chinese medicine, has exhibited promising results in treating vitiligo over an extended period. However, the precise underlying mechanism of its action remains elusive.

Methods: Employing a comprehensive network pharmacology approach, this study identified active compounds and their corresponding targets within LDF, while also pinpointing vitiligo-associated targets sourced from the TCMSP database, OMIM, DisGenNET, and Genecards. A network was established to illustrate the connections between active compounds and targets, alongside a protein-protein interaction network. Further analyses, encompassing Gene Ontology (GO) function and KEGG pathway enrichment, were conducted using the DAVID platform. Molecular docking simulations were performed utilizing AutoDockTools and AutoDockVina software. To validate the outcomes of the systematic pharmacological investigation, experiments were conducted using juvenile zebrafish.

Results: The collective effort of the network pharmacology approach yielded a compilation of 41 compounds and 192 targets. Molecular docking simulations notably revealed the lowest binding energies for CAT-quercetin and CAT-Kaempferol interactions. The utilization of juvenile zebrafish experiments highlighted a significant increase in melanocyte count following methoxsalen and LDF treatment. Notably, LDF prominently augmented the expression levels of proteins related to melanogenesis. Additionally, LDF showcased the capacity to enhance CAT and SOD levels while concurrently reducing ROS and MDA activity. In contrast to the model group, substantial increases in protein and mRNA levels of Nrf2 and HO-1 were observed in response to LDF treatment ($P < 0.05$).

Conclusion: Through a meticulous network pharmacology approach, this study successfully predicted active components and potential targets associated with LDF's application in vitiligo treatment. The therapeutic effectiveness of LDF against vitiligo is postulated to stem from its regulation of oxidative stress factors and the Nrf2/HO-1 pathway.

* Corresponding author. School of Traditional Chinese medicine, Southern Medicial University, No.1023, South Shatai Road, Baiyun District, Guangzhou, Guangdong, 510515, China.
E-mail address: julietdy@smu.edu.cn (Y. Deng).

https://doi.org/10.1016/j.heliyon.2023.e21744
Received 25 June 2023; Received in revised form 29 August 2023; Accepted 26 October 2023
Available online 28 October 2023

1. Introduction

Vitiligo, a prevalent and persistent skin condition, is characterized by the gradual loss of pigmentation in both skin and mucosal tissues. This disheartening disorder affects approximately 1 % of the global population [1]. The conspicuous presence of the disease on patients' skin not only takes a physical toll but also significantly disrupts their daily life and professional commitments. Consequently, individuals grappling with this condition often experience profound psychological distress.

While the treatment approach for vitiligo is often tailored to each individual's specific needs, there are certain overarching strategies. For instance, in more advanced stages, the utilization of glucocorticoids emerges as a common choice, effectively minimizing the progression of depigmented areas. During the acute phase, topical glucocorticoids along with calcineurin inhibitors like tacrolimus and pimecrolimus prove beneficial. During the stable phase, therapies such as narrow-band ultraviolet phototherapy are employed. In cases where vitiligo presents a formidable challenge, techniques like skin grafting can be considered [2,3]. It's worth noting that despite these approaches, current vitiligo treatments are characterized by their time-intensive nature, high costs, and often suboptimal efficacy.

At present, Traditional Chinese Medicine (TCM) is gradually being applied to the prevention and treatment strategy of a variety of diseases, and receiving considerable attention in treatment of vitiligo. Compared with conventional treatment regimens, the long-term application of TCM has less toxicity and minor side effects, therefore, TCM is becoming increasingly popular among patients with vitiligo [4–6].

Liuwei Dihuang formula (LDF) is a classical TCM herbal formula consisting of six herbs: Prepared Rehmannia Root (*Radix Rehmanniae Praeparata*), Medical Dogwood (*Cornus officinalis Sieb. et Zucc.*), Chinese yam (*Rhizoma Dioscoreae*), Oriental Waterplantain Rhizome (*Alisma plantago-aquatica Linn*), indian bread (*Wolfiporia cocos (F.A. Wolf) Ryvarden & Gilb.*), Tree Peony Bark (*Moutan Cortex*). It has been clinically proved that Liuwei Dihuang, a representative formula for nourishing the liver and kidney, can treat both depigmentation skin disease vitiligo and hyperpigmentation skin disease chloasma, it had significant advantages in the treatment of pigment disorders, and can improve the pathological alterations of abnormal increase or decrease of pigment [7,8]. The bi-directional metabolic regulation of Liuwei Dihuang formula on melanin has been verified in experimental models such as mouse B16 melanoma cells and human primary cultured normal melanocytes [9,10]. And our previous study showed that Liuwei Dihuang formula can promote the proliferation and melanin synthesis of human normal melanocytes cultured in vitro, and the same time the serum containing Liuwei Dihuang formula can up regulate tyrosinase activity in melanocytes and mouse models [11–13].

However, owing to the diversity of chemical components of traditional Chinese medicine, it is difficult for traditional experimental research to elaborate the mechanism of Liuwei Dihuang formula on melanin metabolism as a whole. Recently a new method to study the mechanism of action of traditional Chinese medicine has appeared, network pharmacology has been extensive used in the study of various traditional Chinese medicine compounds, providing a new research idea for the complex components and mechanism of traditional Chinese medicine. Via widely application of network pharmacology, this study screened the monomeric components of Liuwei Dihuang formula for the treatment of vitiligo with melanin metabolism disorder, established a network model of effective components for the treatment of disease, looked for the active compounds in the formula that promote the formation of melanin, and experimental validation to explore the mechanism of Liuwei Dihuang by molecular docking technology, zebrafish model and molecular biology experiment.The flow path of our study is displayed in Fig. 1.

2. Materials and methods

2.1. Active ingredients database construction of LDF and screening

Compounds of the each herb in LDF were obtained through Traditional Chinese Medicine System Pharmacology Databasetcmsp (TCMSP) (http://tcmspw.com/). According to the characteristics of drug absorption, distribution, metabolism and excretion (ADME) evaluation system, in which the oral bioavailability (OB) $\geq$ 30 % and the drug likeness (DL) $\geq$ 0.18 were set to be the thresholds values for screening the active ingredients and import the active ingredients into the TCMSP for obtaining the targets of each active compounds with probability $\geq$0.15. And then input the targets into UniProt protein database (https://www.uniprot.org), "Home sapiens" and "reviewed" were used as screening conditions to standardize the protein targets of compounds. All the action targets of the active ingredients in Liuwei Dihuang formula were sorted out, and the active ingredient targets network was constructed by using Cytosape 3.9.0 software.

2.2. Collection and screening vitiligo related targets

In order to obtain the information of disease-associated target genes comprehensively, with "vitiligo" as the key word to screen the targets related to vitiligo in the following disease databases: Genecards (https://www.genecards.org)、OMIM (https://omim.org)、DisGeNET (http://www.disgenet.org). And the obtained targets were standardized through the UniProt protein database (https://www.uniprot.org), which collected the genes information of targets after removing duplicates.

2.3. "Herbal-Compound-Disease-Target" network construction

Via Venn 2.1 (https://bioinfogp.cnb.csic.es/tools/venny/) , taking the intersection of targets of active compounds and vitiligo to

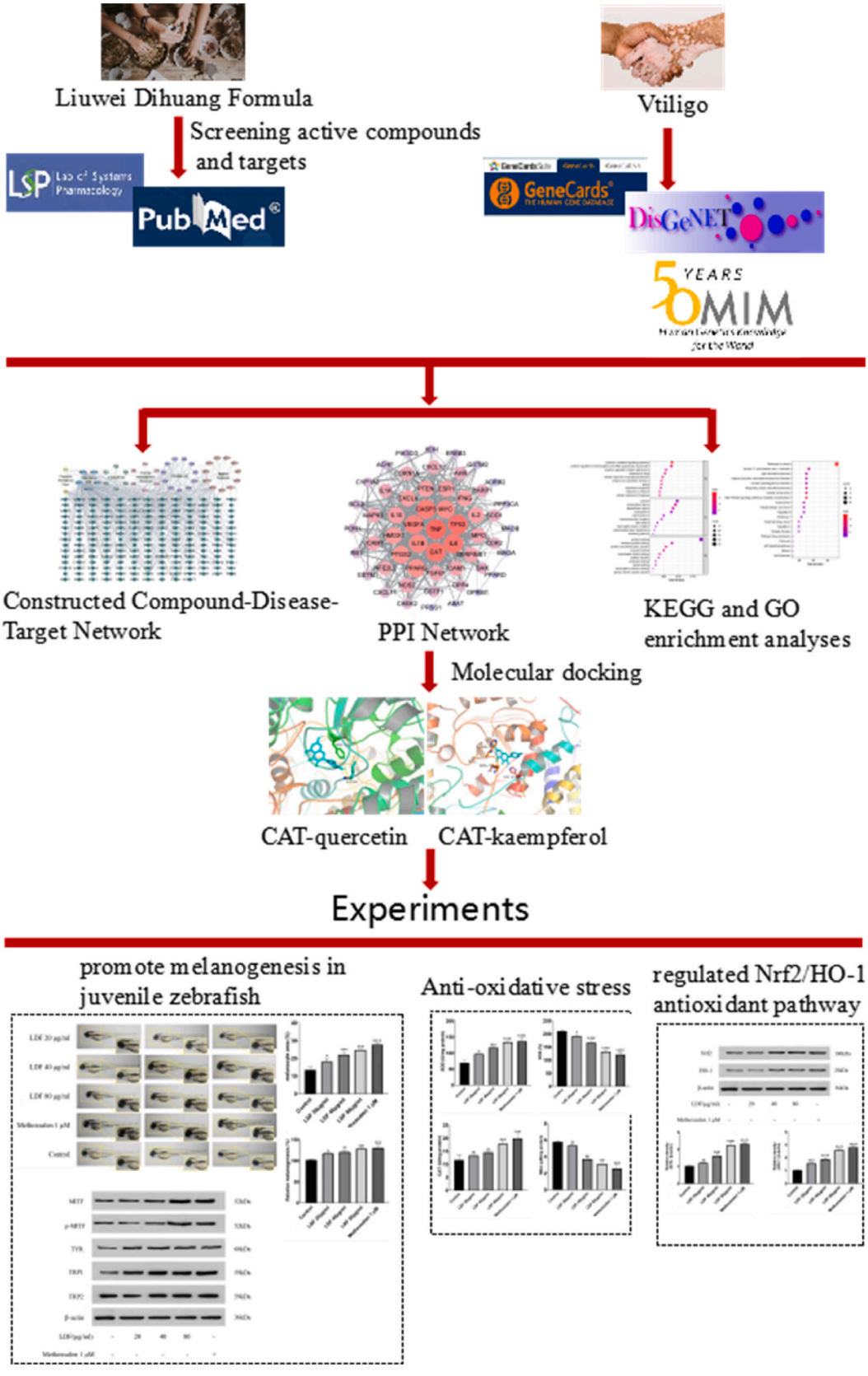

(caption on next page)

Fig. 1. Technical strategy of the current study.

obtain the action targets of Liuwei Dihuang formula for the treatment of vitiligo. The network topology of intersecting targets was analyzed by using Cytoscape 3.9.0 software, and constructed the network diagram of "Herbal-Compound-Disease-Target".

2.4. Construction of protein-protein interaction (PPI) network

Imported common targets into String database (https://string-db.org) to obtain the visualization of PPI network, selected "multiple proteins", the species were limited to *Homo sapiens*, and the PPI medium confidence score >0.4 was the filtering parameter recommended by String database. Download the protein TSV format file, imported it into Cytoscape 3.9.0 software for visualization, screening the core targets with cytohubba plug-in, and constructed the protein interaction network. Nodes and edges represent candidate targets and protein-protein interactions in the PPI network, respectively. In this study, the core target proteins were selected and identified by the parameter "Degree". Degree was used to evaluate the topological importance of the nodes in the network.

2.5. KEGG and GO enrichment analyses

In order to obtain key pathways of LDF treating vitiligo, the Database for Annotation, Visualization and Integrated Discovery (DAVID; version 6.8; https://david.ncifcrf.gov) was used to conduct the gene ontology (GO) and the Kyoto Encyclopedia of Genes and Genomes (KEGG) Pathway Enrichment Analysis. Biologic Process (BP), Molecular Function (MF), and Cell Component (CC) are the general modules that are included in GO term enrichment. The results were visualized by website (bioinformatics.com.cn). Finally, the active component-target-pathway interaction network diagram is drawn by Cytoscape3.9.0. Results with $P < 0.05$ were destined for further analysis.

2.6. Molecular docking to verify the core target

To screen the main effective components and targets of Liuwei Dihuang formula for promoting melanogenesis, using the small organic molecules and information on their biological activities database PubChem (https://pubchem.ncbi.nlm.nih.gov/) to obtain the structure file of ligand small molecule, and construct the 3D structure of the compound with ChemOffice software, save it in *mol2 format and minimize its energy. The crystal structures were of hub target genes screened from the RSCB Protein Data Bank database (PDB) (https://www.rcsb.org/). The water molecules and ligand small molecules in the downloaded protein molecules are removed by the visualization software PyMOL, AutodockTools 1.5.6 was used to open the ligand molecule, hydrogenation, gasteiger charge on the receptor protein molecules, detection of ligand root, search and definition of rotatable bond, and finally save it in pdbqt format. The software AutoDock 4.0 was used to perform molecular docking. Each compound's docked conformation was ranked into clusters according to the binding energy, and the top-ranked conformations whose position with the lowest binding energy (as the most suitable conformation) was selected to be visually analyzed by using Discovery Studio 4.5.

2.7. Main reagents and instruments

MS-222 (sigma, USA); Methylcellulose (sigma, USA); RNase free water, (Takara); Fastpure cell/Tissue Total RNA Isolation Kit (Vazyme Biotech Company Ltd., Nanjing, Jiangsu, China); Strong cracking liquid Ripa (biyuntian, China); BCA protein Assay Kit (Pierce Thermo-Scientific, Rockford, IL, USA); Polyvinylidene fluoride membranes (Millipore, Bedford, MA, USA); Ethanol (sigma, USA, art. No. 270741); Isopropanol (sigma, USA, art. No. 34863); Chloroform (Shanghai McLean Biochemical Technology Co., Ltd., Article No. t819817); the MDA, SOD, CAT, and ROS content in the tissue of zebrafish was determined by detection kit (KeyGen Biotech. Co., Nanjing, China) in accordance with the instructions; Prime script RT Master Mix (perfect real Takara, rr036a); SYBR ® Premix ex taqtm II (TII RNaseH Takara, rr820b); Primers were purchased from Shanghai Sangong Bioengineering Co., Ltd. see attached Table 1 for primer sequence.

Liuwei Dihuang formula were purchased from the pharmaceutical factory of Beijing Tongrentang science and Technology Development Co., Ltd., 120 Capsules/bottle, production batch No. 0073716.

2.8. Preparation of LDF

Liuwei Dihuang formula was prepared by Beijing Tongrentang science and Technology Development Co., Ltd. In brief, 12 g Prepared Rehmannia Root, 12 g Medical Dogwood, 12 g Chinese yam, 12 g Oriental Waterplantain Rhizome, 12 g indian bread, 12 g Tree Peony Bark were decocted in 1200 ml and 900 ml of water twice for each 0.5 h. The decoction was combined, filtered and concentrated to 150 ml. After cooling, the decoction was mixed with same amount of ethanol and the mixture was kept for more than 24 h. The supernatant was filtered and the filtrate was concentrated to 10–15 ml. After 40 g of the mixture of sucrose:dextrin (3:1) was added, the mixture was granulated, dried and sieved with a 12 mesh sieve to obtain the Liuwei Dihuang formula pills. LDF was diluted with distilled water to concentrations of 20, 40, and 80 μg/ml. All solutions were stored at 4 °C until use.

2.9. Establishment of juvenile zebrafish melanin regeneration model and drug administration

AB strain zebrafish were obtained from CZRC (China Zebrafish Resource Center, CZRC) (http://www.zfish.cn/) and cultured in the zebrafish culture system with light: dark = 14:10 cycle at the constant temperature of 25 °C–28 °C. Embryos from natural spawning were collected in embryo medium (5 mM NaCl, 0.17 mM KCl, 0.33 mM $CaCl_2$, 0.33 mM $MgSO_4$, 0.7 mM HEPES, with distilled water, pH 7.2, supplemented with 1 % methylene blue). The male and female fish are placed in the spawning pond in the ratio of 2:3. Within 30 min after spawning, collect the embryos in egg water and put them into the incubator. The temperature is maintained at 28.5 ± 0.5 °C. Egg water was changed 2–3 times within 24 hpf (24 h post-fertilization). Then, the culture medium was replaced with LDF (20–80 μM), methoxsalen (1 μM) was used as a positive control. Zebrafish embryo medium (3000 μl) was added to each well of a six-well plate, followed by adding 10 embryos. After 1 h, replaced with LDF (0–120 μM), methoxsalen (1 μM), the survival rate of embryos was observed for the next 48 h. The dead embryos were removed from the well after 24 and 48 h and calculated survival rate of embryo.

2.10. Measure the area of melanocytes in specific parts of zebrafish head

Spontaneous melanin content was measured from zebrafish larvae at 3 day post-fertilized (dpf). The zebrafish larvae were administrated with LDF (20–80 μM) and methoxsalen (1 μM) after 24hpf, and washed away after 72 h, anesthetizing zebrafish larvae in 3-Aminobenzoic acid ethyl ester methanesulfonate (MS-222) for about 5–10min, the larvae were mounted in 2 % methyl cellulose on a depression slide, and images were collected using an Olympus SZ2-ILST stereomicroscope (Tokyo, Japan). The densitometric analysis was performed using Image J software (National Institute of Health, Bethesda, MD). The quantification of pigmentation data was calculated as the percentage in comparison with the untreated control.

2.11. Determination of melanin content in juvenile zebrafish

Zebrafish were washed twice with egg water after drug treatment group and experimental group. Take 10 live juveniles randomly from each group, add them into 2 ml EP tube, and suck up the liquid as much as possible. Add 200 μl Ripa lysate per tube, smash the tissue. The process needs to be operated on ice. Centrifuge at 4 °C 13,000 rpm for 10 min, and suck all the liquid from the upper layer after centrifugation. Add 600 ml of 1 mol/l NaOH to each EP tube and treat with metal bath at 100 °C for 30 min. Shake up the liquid and transfer it to 96 well plate. Each group is provided with 2 double holes, 200 μl/hole. The OD value of 490 nm was measured by microplate reader. The maximum and minimum values of each concentration group are removed and then the average value is removed. Relative melanin content = (absorbance value of drug group/absorbance value of blank concentration group) × 100 %. All experiments were repeated three times.

2.12. RNA extraction and quantitative reverse transcription polymerase chain reaction

At 96 hpf, zebrafish larvae of control and LDF-treated groups were collected for RNA isolation. Total RNA was extracted from 20 zebrafish larva using Fastpure cell/Tissue Total RNA Isolation Kit (Vazyme Biotech Company Ltd., Nanjing, Jiangsu, China) following the manufacturer's protocol. cDNA was synthesized using a Primescript RT Master Mix (perfect real Takara, rr036a); SYBR ® Premix ex taqtm II (TII RNaseH Takara, rr820b). A real-time PCR assay was performed using SYBR ® Premix ex taqtm II (TII RNaseH Takara, rr820b); Primers were purchased from Shanghai Sangong Bioengineering Co., Ltd. The sequence of the sense and antisense primers were shown in Table 1.

2.13. LDF stimulates expression of MITF, p-MITF, tyrosinase, TRP1 and TPR2

Western blotting was carried out in accordance with the relevant standard techniques. The total protein of zebrafish tissues homogenate were extract using RIPA lysis buffer. The supernatants were collected by centrifugation at 12,000×*g* for 30 min at 4 °C. The BCA protein Assay Kit was used to quantify the protein concentration. For WB, 40 μg protein was loaded and run on an 8 % SDS-PAGE gel. The protein bands were transfer by using Polyvinylidene fluoride membranes. 5 % BSA solution preparation with TBST was used to block the membrane for 1h at room temperature, and then incubated with primary antibodies at 4 °C overnight. The primary antibodies used in the study were as follows: Anti-MITF (Abcam, ab215845), Anti-TRP1 (Abcam, ab235447), Anti-TRP2 (Abcam, ab221144), p-MITF antibody was purchased from Affinity Biosciences (AF3027), TYR antibody (CST, 8954S), Anti-Nrf2 (CST,

Table 1
Primer sequences for real-time PCR.

Gene name	Primer sequence (5′–3′)		Product (bp)	GenBank serial number
Nrf2	Forward	GGTTGCCCACATTCCCAAATC	119	NM_001313901.1
	Reverse	CAAGTGACTGAAACGTAGCCG		
HO-1	Forward	TTCAAGCAGCTCTACCGCTC	90	NM_002133.2
	Reverse	GAACGCAGTCTTGGCCTCTT		
GAPDH	Forward	GGACTCATGACCACAGTCCAT	109	NM_000194.2
	Reverse	CAGGGATGATGTTCTGGAGAG		

12721S), and Anti–HO–1 (CST, 26416S) antibodies were purchased from Cell signaling Technology. After washing three times in Tris-buffered saline containing 0.1 % Tween-20 at pH 7.6 (TBST), the membranes were incubated with the appropriate secondary antibody (1:4000), Anti-rabbit IgG, HRP-linked Antibody #7074 and Anti-mouse IgG, HRP-linked Antibody #7076, which were purchased from Cell Signaling Technology, Inc. Quantification of the bands was performed by measuring the signal intensity using Image-Pro Plus (version 6.0) and normalizing them to the signal of the housekeeping β-Actin antibody.

2.14. Detection kit to test oxidative stress factors

After administration with different concentration of LDF and methoxsalen for 72 h, 150 zebrafish larvae in each group were pooled together in centrifuge tubes and homogenized on ice-cold saline (1 g of tissue in 9 ml of normal saline). The supernatants were collected for analysis of anti oxidative enzyme activities and lipid peroxidation after centrifugation at 3500 rpm for 15 min at 4 °C. Reactive oxygen species (ROS, E004-1-1), Superoxide dismutase (SOD, A001-1-2), Malondialdehyde (MDA, A003-1-2), Catalase (CAT, A007-1-2), levels were measured by assay kits which were purchased from Nanjing Jiancheng (Nanjing, China).

2.15. Statistical analysis

The results were presented as mean ± standard deviation (‘x ± s). The significance was determined by using one-way analysis of variance (ANOVA) followed by Dunnett’s post-hoc test, using GraphPad Prism 6 (La Jolla, CA, USA) and SPSS 22 (IBM, Armon, NY, USA). Significant differences compared with the control were identified when the *P* value was less than 0.05. All the experiments were performed in triplicate.

3. Results

3.1. Screening active targets of LDF and targets vitiligo

After ADME screening via TCMSP database, removing the compounds that could not find the relevant targets, 41 unduplicated compounds and 192 unduplicated targets were obtained, which included 475 compound-target relationships. The active ingredient-target network diagram was constructed by Cytoscape3.9.0. The network involves 239 nodes (6 traditional Chinese medicines, 41 compounds and 192 drug targets) and 475 edges, each edge represents the interaction between the compound and target (Fig. 2A). Among five botanical drugs of Prepared Rehmannia Root, Medical Dogwood, Chinese yam, Oriental Waterplantain Rhizome, indian bread and Tree Peony Bark corresponded to 2, 13, 12, 7, 6 and 6 compounds, respectively, the general information of the active compounds of LDF is shown in Table 2. We found a potential synergistic effect of these six botanical drugs in the target level without many overlaps in the compound level.

A total of 650 vitiligo-related proteins were obtained from Genecards, OMIM, DisGeNET and other disease databases and 56 common targets of active components and vitiligo were screened by Venn2.1.0 software, as shown in Fig. 2B. The network of vitiligo and the active ingredient of LDF, was constructed by Cytoscape3.9.0 software, showed in Fig. 2C.

3.2. PPI network construction and screening key targets

After screening all of the compounds and targets, we want to recognize the potential corresponding compounds and targets of LDF anti-vitiligo effect. Based on String and Cytoscape3.9.0 software, the PPI network was constructed consisting of 55 protein nodes and 555 edges, and the core targets were screened by cytohubba plug-in. The edges represent the interaction between proteins. The more connections, the greater the correlation. The size and color of the nodes represent the Degree value, the deeper the color and the larger the size of nodes, represents the larger the Degree value. The weight of the edge represents the combines core value (Fig. 3). According to the properties of network topology, compounds and drug targets which connected with nodes may play a core role in the whole network. The top 10 key proteins according to the Degree value include TNF, TP53, CAT, IL6, CASP3, VEGFA, IL1B, MYC, PPARG and PTGS2, as shown in Table 3.

3.3. Functional enrichment analysis

GO analysis of the potential therapeutic target genes was performed using the DAVID database. The x-axis indicates the number of genes enriched in that term. The redder the color, the smaller the value of *P* adjust (FDR); it also denotes greater credibility and greater importance. In contrast, the bluer the color, the greater is the value of *P* adjust. For a brief demonstration, we intercepted the top 10 terms of GO analysis and the KEGG metabolic pathway of the top 20 from small to large according to the *P*-value. (Fig. 4A). The y-axis represents GO terms. The x-axis indicates the number of genes enriched in that term. The redder the color, the smaller the *P*-value; it also denotes greater credibility and greater importance. The results indicated that target genes were mostly enriched in cytokine-mediated signaling pathway, response to drug, cellular response to lipopolysaccharide in Biological Process (BP); extracellular region, macromolecular complex, mitochondrion in Cell Composition (CC) analysis; enzyme binding, protein homodimerization activity, identical protein binding, and cytokine activity in Molecular Function (MF). The result of KEGG pathway enrichment analysis indicated that target genes were significantly enriched in pathways in GE-RAGE signaling pathway, fluid shear stress and atherosclerosis, and Lipid and atherosclerosis (Fig. 4B).

3.4. Molecular docking

Quercetin and kaempferol are bioflavonoids. Many studies have shown that quercetin and kaempferol have good anti-inflammatory and antioxidant effects [14–18]. According to the results of network pharmacological analysis, kaempferol and quercetin are one of the effective components in the LDF, while the differentially expressed hub gene catalase (CAT), as a downstream crucial regulatory target, is closely related to the pathogenesis of vitiligo. Among the calculated binding energies of various compounds, the binding energies of CAT-quercetin and CAT-kaempferol are the lowest, indicating that the binding activity is better. Therefore, kaempferol and quercetin were selected for virtual molecular docking with CAT, as shown in Fig. 5.

3.5. LDF promote melanogenesis in juvenile zebrafish

Before the investigation of melanogenesis, a toxicity assay was performed to determine the optimal avirulence concentration of LDF to zebrafish. As shown in Fig. 6A, there was no difference in survival rate of embryo when the concentration were 0, 20, 40 and 80 μg/ml of LDF, and these concentration had no significantly toxicity observed in embryos. Methoxsalen is a drug that has been historically used in the treatment of vitiligo. Our previous research found that there was no statistically significant difference in the survival rate of zebrafish embryos under 1 μM methoxsalen compared to the control group, and it could significantly increase the melanocyte area of

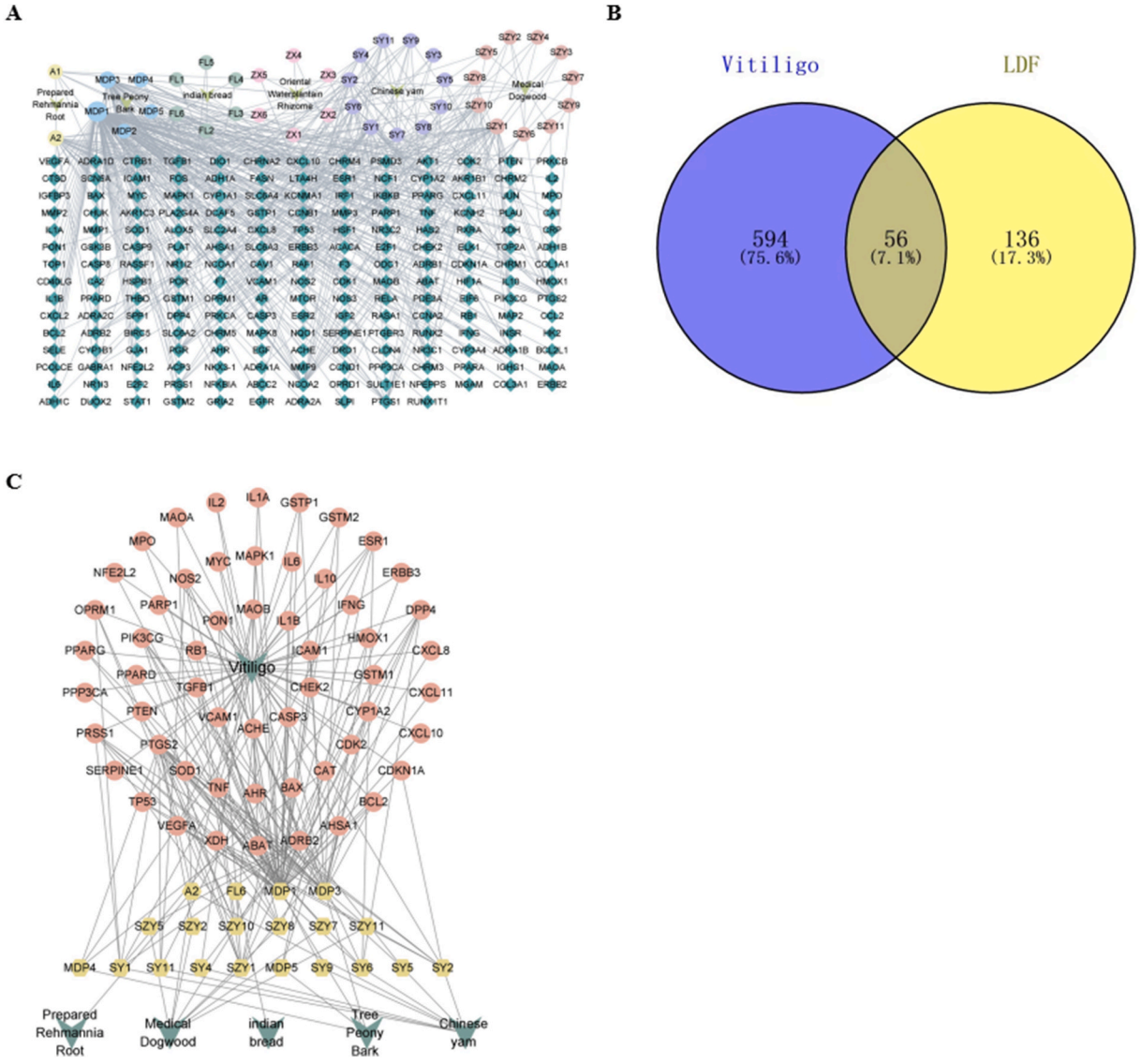

Fig. 2. Constructed compound-disease-target network. A. LDF-active ingredients-target network; B. LDF-Vitiligo-common target Venn diagram; C. LDF-Vitiligo-target network.

zebrafish head. Zebrafish juvenile were administrated with 1 μmol/L methoxsalen and 20 μg/ml, 40 μg/ml, 80 μg/ml LDF respectively for 72 h. The results showed that compared with the control group, the melanocyte area of zebrafish head observably increased after treated with methoxsalen and LDF, while the concentration was 20 μg/ml, the melanocyte area showed no significant difference, and LDF promoted the melanogenesis in juvenile zebrafish, and its effect was similar to that of the methoxsalen group compared with the control group. Moreover, the relative melanogenesis after administration with different concentration of LDF and methoxsalen were increased compared with control group, the difference was statistically significant ($P < 0.01$; Fig. 6B–D). In addition, we further refined our exploration accordingly, the juvenile zebrafish were exposured to LDF at different concentrations, the expression levels of melanogenesis-related protein: microphthalmia-associated transcription factor (MITF), phosphorylation microphthalmia-associated transcription factor, tyrosinase (TYR), tyrosinase-related protein 1 (TRP1), tyrosinase-related protein 2 (TRP2), were measured. As shown in the results, the levels of TYR and TRP1 proteins were significantly increased with the administration of the LDF (20 μg/ml, 40 μg/ml, 80 μg/ml) and methoxsalen ($P < 0.05$), whereas MITF, p-MITF and TRP2 expression level showed no difference with the

Table 2
Active compounds in LDF.

Herbs	number	Mol ID	Molecule Name	OB (%)	DL
Prepared Rehmannia Root	A1	MOL000359	sitosterol	36.91	0.75
	A2	MOL000449	Stigmasterol	43.83	0.76
Medical Dogwood	SZY1	MOL000358	beta-sitosterol	36.91	0.75
	A1	MOL000359	sitosterol	36.91	0.75
	A2	MOL000449	Stigmasterol	43.83	0.76
	SZY2	MOL001494	Mandenol	42	0.19
	SZY3	MOL001495	Ethyl linolenate	46.1	0.2
	SZY4	MOL001771	poriferast-5-en-3beta-ol	36.91	0.75
	SZY5	MOL002879	Diop	43.59	0.39
	SZY6	MOL002883	Ethyl oleate (NF)	32.4	0.19
	SZY7	MOL005503	Cornudentanone	39.66	0.33
	SZY8	MOL005530	Hydroxygenkwanin	36.47	0.27
	SZY9	MOL005531	Telocinobufagin	69.99	0.79
	SZY10	MOL008457	Tetrahydroalstonine	32.42	0.81
	SZY11	MOL005481	2,6,10,14,18-pentamethylicosa-2,6,10,14,18-pentaene	33.4	0.24
Chinese yam	SY1	MOL000322	Kadsurenone	54.72	0.38
	A2	MOL000449	Stigmasterol	43.83	0.76
	SY2	MOL000546	diosgenin	80.88	0.81
	SY3	MOL000953	CLR	37.87	0.68
	SY4	MOL001559	piperlonguminine	30.71	0.18
	SY5	MOL001736	(−)-taxifolin	60.51	0.27
	SY6	MOL005430	hancinone C	59.05	0.39
	SY7	MOL005435	24-Methylcholest-5-enyl-3belta-O-glucopyranoside_qt	37.58	0.72
	SY8	MOL005438	campesterol	37.58	0.71
	SY9	MOL005440	Isofucosterol	43.78	0.76
	SY10	MOL005458	Dioscoreside C_qt	36.38	0.87
	SY11	MOL005465	AIDS180907	45.33	0.77
Oriental Waterplantain Rhizome	A1	MOL000359	sitosterol	36.91	0.75
	ZX1	MOL000831	Alisol B monoacetate	35.58	0.81
	ZX2	MOL000849	16β-methoxyalisol B monoacetate	32.43	0.77
	ZX3	MOL000853	alisol B	36.76	0.82
	ZX4	MOL000856	alisol C monoacetate	33.06	0.83
	ZX5	MOL002464	1-Monolinolein	37.18	0.3
	ZX6	MOL000862	[(1S,3R)-1-[(2R)-3,3-dimethyloxiran-2-yl]-3-[(5R,8S,9S,10S,11S,14R)-11-hydroxy-4,4,8,10,14-pentamethyl-3-oxo-1,2,5,6,7,9,11,12,15,16-decahydrocyclopenta [a] phenanthren-17-yl]butyl] acetate	35.58	0.81
indian bread	FL1	MOL000273	(2R)-2-[(3S,5R,10S,13R,14R,16R,17R)-3,16-dihydroxy-4,4,10,13,14-pentamethyl-2,3,5,6,12,15,16,17-octahydro-1H-cyclopenta [a]phenanthren-17-yl]-6-methylhept-5-enoic acid	30.93	0.81
	FL2	MOL000275	trametenolic acid	38.71	0.8
	FL3	MOL000279	Cerevisterol	37.96	0.77
	FL4	MOL000282	ergosta-7,22E-dien-3beta-ol	43.51	0.72
	FL5	MOL000283	Ergosterol peroxide	40.36	0.81
	FL6	MOL000296	hederagenin	36.91	0.75
Tree Peony Bark	MDP1	MOL000098	quercetin	46.43	0.28
	MDP2	MOL000211	Mairin	55.38	0.78
	A1	MOL000359	sitosterol	36.91	0.75
	MDP3	MOL000422	kaempferol	41.88	0.24
	MDP3	MOL000492	(+)-catechin	54.83	0.24
	MDP3	MOL007374	5-[[5-(4-methoxyphenyl)-2-furyl]methylene]barbituric acid	43.44	0.3

treatment of 20 μg/ml LDF, and as up the administration dose, the expression level gradually increased (Fig. 6E). The results indicated that LDF can promote melanogenesis and up-regulate the expression of melanogenesis-related genes.

3.6. LDF regulates levels of oxidative stress factors

According to the results of network pharmacological analysis, showed that the catalase (CAT), one of the differentially expressed hub genes in the LDF treatment with vitiligo. To investigate the mechanisms of LDF therapeutical effect to vitiligo, so we further detected the activities of oxidative stress indexes ROS, SOD, MDA and CAT in the tissue of juvenile zebrafish. As shown in Fig. 7, compared with the control group, after administration of LDF (40 μg/ml and 80 μg/ml), the level of ROS and MDA decreased and the activities of SOD and CAT increased in juvenile zebrafish, whereas, the concentration was lower 40 μg/ml, the level of CAT, MDA have no significance. Moreover, the concentration of LDF is 80 μg/ml, the content of oxidative stress factors was similar with methoxsalen administration, which suggested that LDF can promotes melanogenesis by regulating the level of oxidative stress factors in juvenile zebrafish.

3.7. LDF up-regulated Nrf2/HO-1 antioxidant pathway

To further reveal the mechanism by which LDF regulates oxidative stress factors, we firstly measured the protein levels of Nrf2/HO-1 antioxidant pathway in juvenile zebrafish. We found that treatment with 20 μg/ml of LDF did not significantly affect the expression of Nrf2 protein, while the administration with 40 μg/ml and 80 μg/ml, the level of these two proteins increased significantly ($P < 0.05$; Fig. 8A). Moreover, we investigated the mRNA levels of Nrf2 and HO-1 in juvenile zebrafish after LDF and methoxsalen treatment. The results showed that compared with control group, Nrf2 and HO-1 expression levels was elevated with the administration of 40 μg/ml and 80 μg/ml LDF, and further increased in methoxsalen-treated group ($P < 0.05$; Fig. 8B).

4. Discussion

Vitiligo is a common depigmentation disease of the skin caused by the disappearance or reduction of the number of melanocytes, which is seriously affecting the quality of patients' life [19,20]. LDF, a well-known traditional Chinese medicine has been proved to be effective in the treatment of vitiligo due to its unique characteristics. However, the molecular mechanism of LDF on vitiligo still remained unclear, that limited its appliance and modernization. Network pharmacology is an creative method, which systematically detects the mechanism of action of traditional Chinese medicine on a variety of diseases [21,22]. In this work, the effects of LDF against vitiligo and its potential pharmacological mechanisms were studied based on network pharmacological analysis and experimental validation. Network analysis identified relevant potential targets (CAT). Then, the molecular docking and in vivo juvenile zebrafish model validation further confirmed that, LDF significantly increased the percentage of melanin area and melanin synthesis in juvenile zebrafish, and increased the protein levels of MITF, p-MITF, TYR, TRP1 and TRP2. At the same time, LDF inhibited levels of oxidative stress factors such as ROS and MDA, and increased the level of SOD and CAT. WB results showed LDF can active the Nrf2/HO-1 pathway. Therefore, inhibiting oxidative stress factors and increasing the synthesis of melanocytes may be the potential mechanism of LDF against vitiligo.

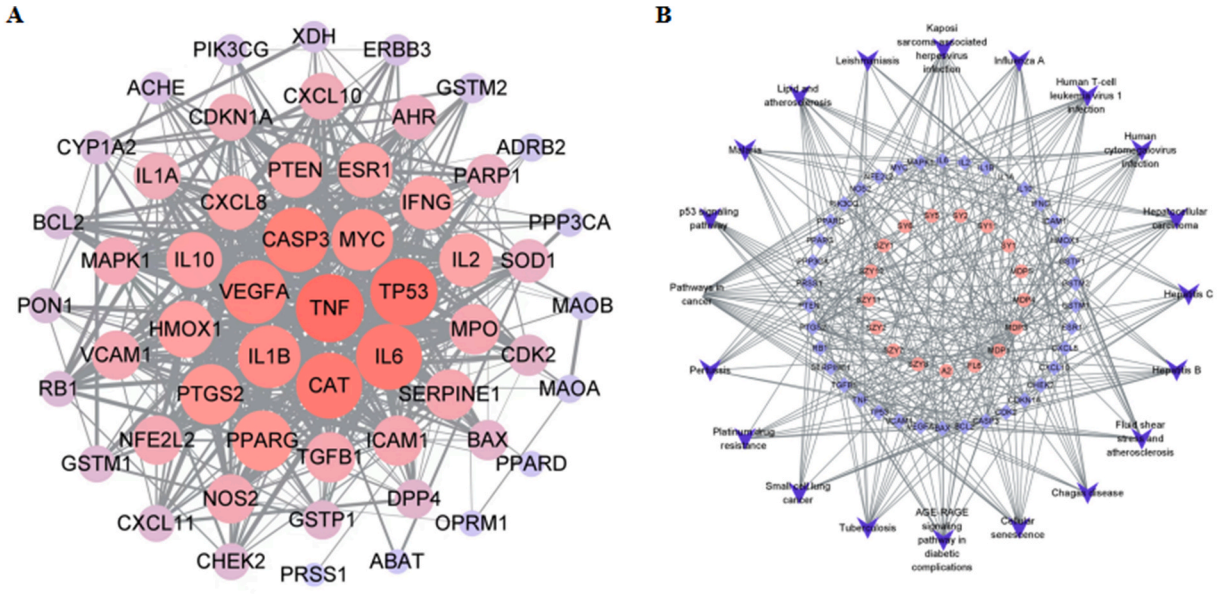

Fig. 3. Screening compoouds-disease core targets. A. LDF-Vitiligo-target PPI network; B. LDF-Vitiligo-core target network.

Table 3
Core targets with top 10° values.

Rank	Name	Degree
1	TNF	41
2	TP53	40
3	CAT	39
3	IL6	39
5	CASP3	38
6	VEGFA	37
7	IL1B	36
8	MYC	35
9	PPARG	34
9	PTGS2	34

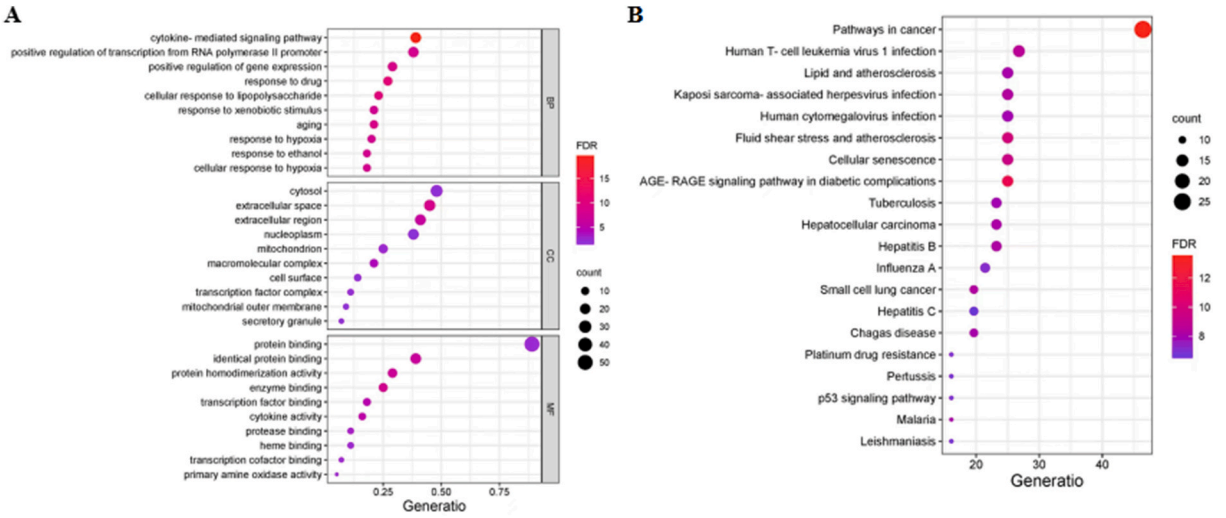

Fig. 4. A. GO-BP, GO-CC, and GO-MF enrichment analysis plots. Only the top 10 GO-terms are displayed in the categories of biological process (GO-BP), cellular component (GO-CC) and molecular function (GO-MF); B. KEGG enrichment analysis. Only the top 20 KEGG-terms are displayed.

Network pharmacological analysis applied to identify the core targets in order to elucidate the basic mechanism of LDF against vitiligo. In this part, according to the analysis of " Active ingredients -vitiligo ", quercetin, kaempferol, sitosterol are the main active components of LDF acting on vitiligo related genes. Modern studies have shown that the incidence of vitiligo is closely related to oxidative stress, and quercetin has a strong antioxidant effect. Animal experiments have shown that quercetin can increase the distribution density and number of melanosomes significantly [23–25]. H_2O_2 can lead to the decrease of melanocyte viability, the change of cell morphology and microstructure, and the occurrence of apoptosis. Cell experiments found that quercetin can avoid oxidative damage caused by H_2O_2 by reducing intracellular ROS, improve cell viability, and reduce the rate of apoptosis [26,27]. Kaempferol is a flavonoid compound with anti-inflammatory, anti-oxidation and anti-cancer effects. Tyrosinase activity was measured in vitro by the mushroom tyrosinase DOPA rate oxidation method. The results showed that the activation rate of 2 mM kaempferol on tyrosinase was

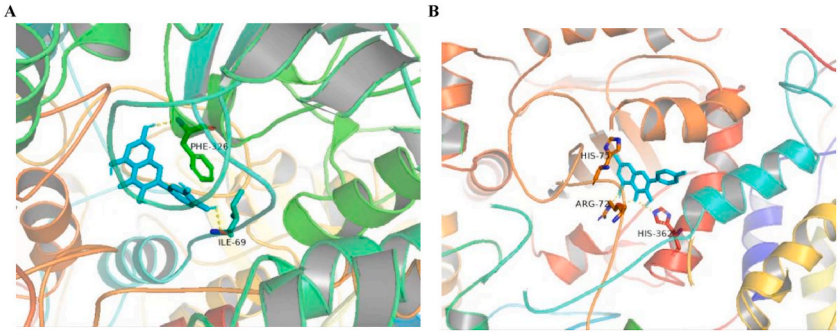

Fig. 5. Molecular docking of quercetin and kaempferol with CAT. A. CAT-quercetin; B. CAT-kaempferol.

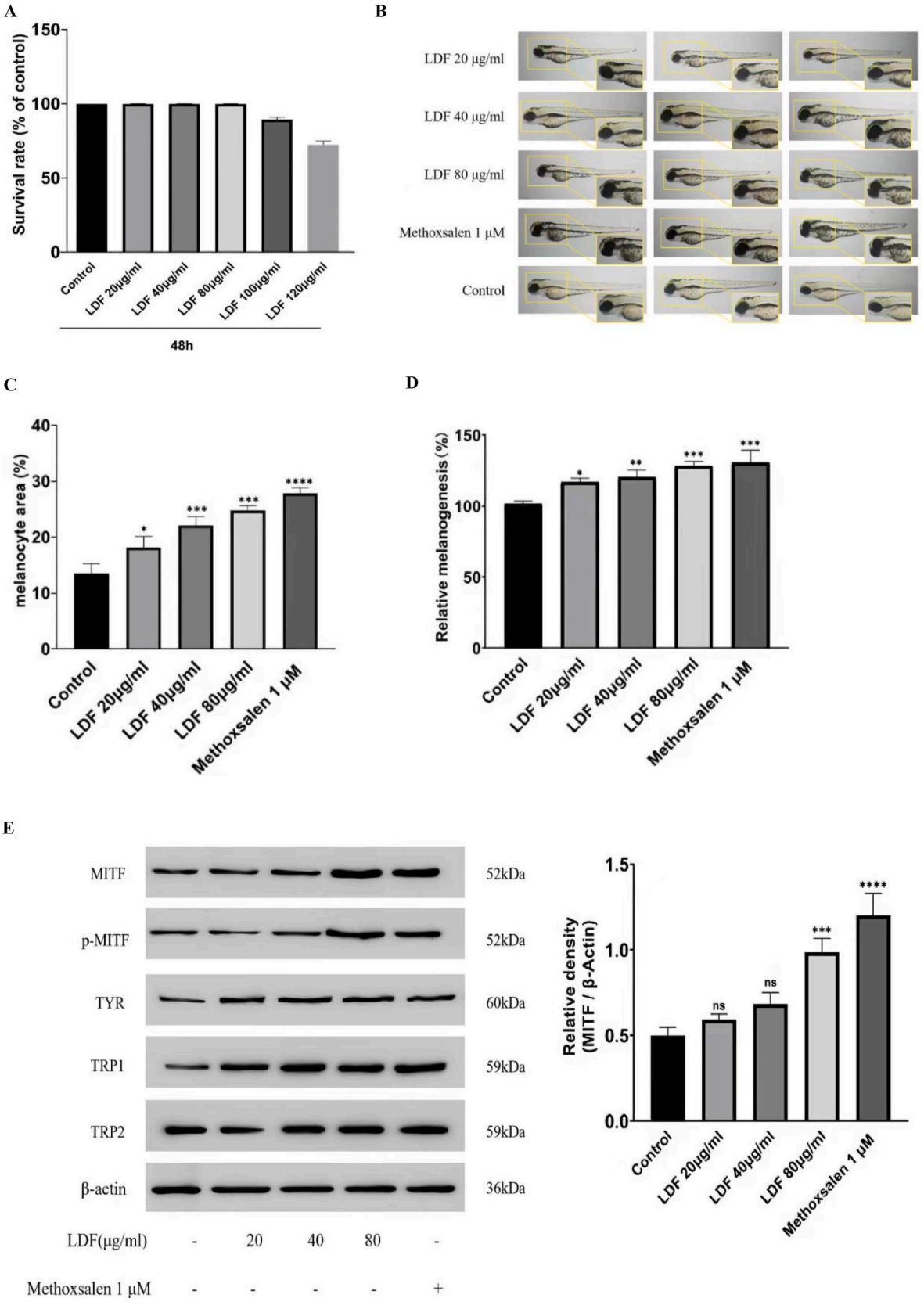
A
Survival rate (% of control)
150
100
50
0
Control
LDF 20μg/ml
LDF 40μg/ml
LDF 80μg/ml
LDF 100μg/ml
LDF 120μg/ml
48h
B
LDF 20 μg/ml
LDF 40 μg/ml
LDF 80 μg/ml
Methoxsalen 1 μM
Control
C
melanocyte area (%)
40
30
20
10
0
Control
LDF 20μg/ml
LDF 40μg/ml
LDF 80μg/ml
Methoxsalen 1 μM
D
Relative melanogenesis (%)
150
100
50
0
Control
LDF 20μg/ml
LDF 40μg/ml
LDF 80μg/ml
Methoxsalen 1 μM
E
MITF
p-MITF
TYR
TRP1
TRP2
β-actin
52kDa
52kDa
60kDa
59kDa
59kDa
36kDa
LDF(μg/ml) - 20 40 80 -
Methoxsalen 1 μM - - - - +
Relative density (MITF / β-Actin)
1.5
1.0
0.5
0.0
ns
ns
Control
LDF 20μg/ml
LDF 40μg/ml
LDF 80μg/ml
Methoxsalen 1 μM

Fig. 6. LDF promote melanogenesis in juvenile zebrafish.
A. Toxicity assays in embryos with drugs administration of LDF (0–120 μg/ml); B. The effect of LDF on melanogenesis with drugs administration of LDF (20–80 μg/ml and 1 μM methoxsalen) for 72 h; C-D. The effect of LDH on melanin contents; E. The effect of LDH on the protein expression of MITF, p-MITF, TYR, TRP1, and TRP2.*, $P < 0.05$; **, $P < 0.01$; ***, $P < 0.001$; ****, $P < 0.0001$ vs Control.

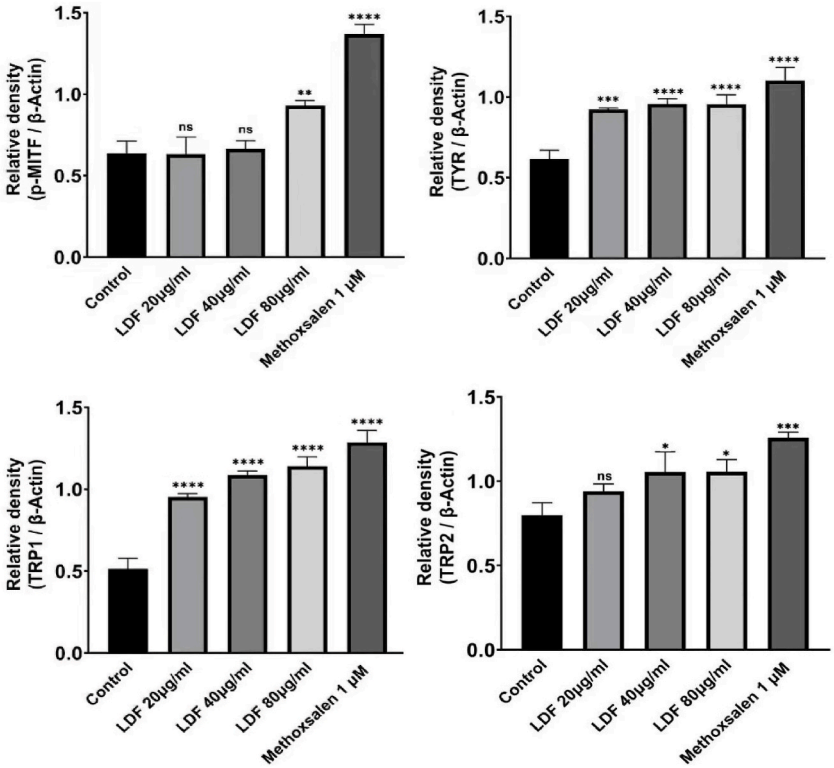

Fig. 6. (*continued*).

as high as 110 % [28]. Our molecular docking results showed that both kaempferol and quercetin could bind to CAT with good activity.

The core targets of LDF active components were identified through PPI network, including CAT、TNF、TP53、IL-6, which are closely related to the process of Oxidative stress pathway. It is found that DNA base oxidative damage is closely related to the pathogenesis of vitiligo [29,30]. Oxidative stress can activate the unfolded protein response of keratinocytes, increase the expression of chemokine CXCL16, and induce $CD8^{+}$T cells to attack melanocytes [31,32]. In addition, the expression of IL-15 in keratinocytes induced by oxidative stress helps to activate $CD8^{+}$T cells, which is a new mechanism to induce autoimmunity in vitiligo [33]. Therefore, antioxidant therapy may protect melanocytes and block autoimmune attack, thus contributing to the treatment of vitiligo. Researchers have studied the effect of oxidative stress on vitiligo and found that compared with the activities of MDA, SOD, GSH and other antioxidant enzymes, oxidative stress has a significant effect on the plasma activity of patients with vitiligo [34,35]. It can be seen that there is an imbalance between oxidation and antioxidation in the plasma of patients with vitiligo, and the imbalance between oxidation and antioxidation in the plasma of patients with advanced vitiligo is more serious than that in the stable phase [36].

Our juvenile zebrafish experiments showed that LDF could significantly reduce the levels of various oxidative stress factors in a dose-dependent manner such as ROS, SOD and MDA; it can increase the level of protective factor CAT simultaneously.

ROS overload significantly impaired melanogenesis [37]. In depigmentation diseases such as vitiligo, unbalanced antioxidant system and uncontrolled ROS overload will damage melanocytes and reduce cell viability. Meanwhile, ROS is cleared [38,39]. It is reported that the activation of Nrf2/ARE antioxidant pathway is the main method for skin cells to scavenge ROS [40,41]. In this experiment, LDF could up regulate the protein and mRNA levels of Nrf2 and HO-1 in juvenile zebrafish, which means that LDF can activate Nrf2/HO-1 pathway. Therefore, we suggest that LDF can protect melanocytes from oxidative stress damage by activating Nrf2/HO-1 antioxidant pathway and scavenging ROS.

There are many Chinese and Western medicine treatment methods for vitiligo, and they all have certain effects. TCM and Western medicine can complement each other's advantages, and maximize the clinical efficacy, which is also the inevitable trend of future medical development [42].

While this study has provided valuable insights into the potential therapeutic effects of Liuwei Dihuang Formula (LDF) on vitiligo and its underlying mechanisms, several limitations should be acknowledged:

In vitro and Zebrafish Model: The study predominantly relied on in vitro analyses and a zebrafish model to investigate the effects of

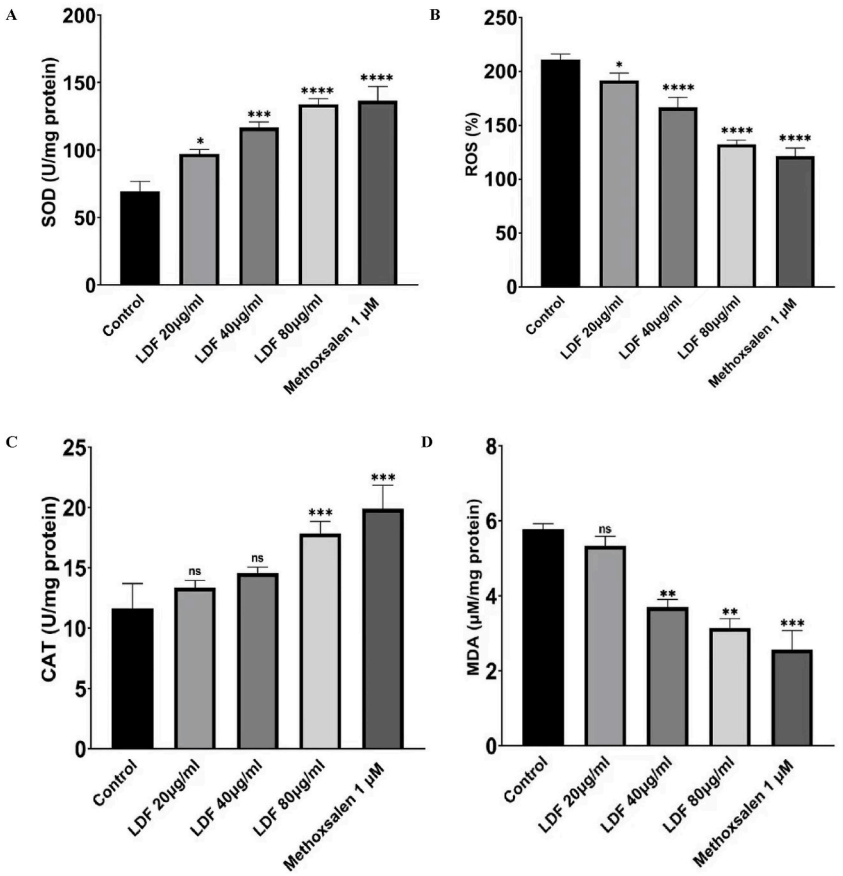

Fig. 7. The effect of LDH on the activity of oxidative stress factors in juvenile zebrafish. A. SOD; B. ROS; C. CAT; D. MDA. *, $P < 0.05$; **, $P < 0.01$; ***, $P < 0.001$; ****, $P < 0.0001$vs Control.

LDF on melanogenesis and oxidative stress. Although these experimental systems offer advantages in terms of cost-effectiveness and ease of manipulation, they do not fully recapitulate the complexity of human physiology and pathophysiology. Further studies using animal models more closely related to human skin pigmentation, such as murine models or ex vivo human skin explants, would be valuable to validate the findings observed in this study.

Network Pharmacology Predictions: The network pharmacology approach used in this study offers a comprehensive way to predict potential interactions between compounds and targets. However, these predictions are based on existing databases and may be subject to errors or incomplete information. Experimental validation of the interactions identified through network pharmacology, such as molecular docking studies, provides additional support but still requires further in-depth investigation. These limitations highlight the need for further research to validate and expand upon the findings presented here. Future studies incorporating more diverse experimental approaches, including clinical trials, and a deeper mechanistic understanding will contribute to a more comprehensive assessment of the therapeutic efficacy of LDF for vitiligo treatment.

5. Conclusion

In a word, this study found that hub genes and some functional biological pathways that involved in the treatment of LDF on vitiligo disease based upon bioinformatics and molecular docking. Then we demonstrated that LDF increasing the synthesis of melanocytes and exerted a significant against vitiligo effect in juvenile zebrafish, the mechanism may be potent via activating the Nrf2/HO-1 pathway and inhibiting the level of oxidative stress factors. These findings provide new potential diagnostic markers and therapeutic targets of LDF.

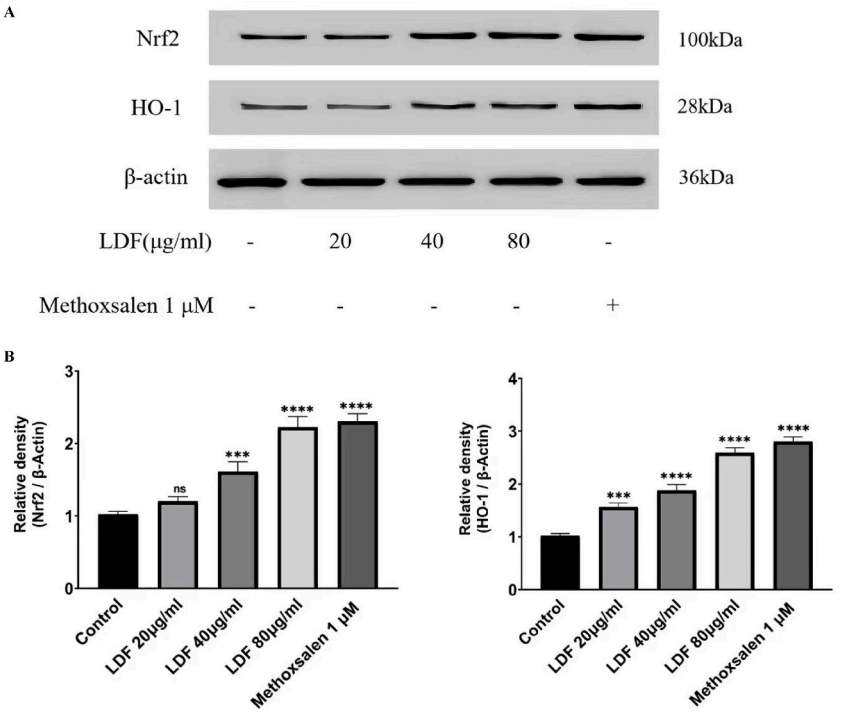

Fig. 8. The effect of LDH on Nrf2/HO-1 signal pathway in zebrafish larvae at 96 hpf. A. The protein level of Nrf2 and HO-1; B. The mRNA levels of Nrf2 and HO-1. *, $P < 0.05$; **, $P < 0.01$; ***, $P < 0.001$; ****, $P < 0.0001$vs Control.

Author contribution statement

Dandan Wang:conceived and designed the experiments; performed the experiments; analyzed and interpreted the data; wrote the paper. Yan Yang:performed the experiments; analyzed and interpreted the data; Gulijiayina Hengerjia:performed the experiments; analyzed and interpreted the data; Yan Deng:conceived and designed the experiments; analyzed and interpreted the data; contributed reagents, materials, analysis tools or data; wrote the paper.

Funding statement

We appreciate all the participants for their exceptional cooperation as well as valuable contributions. This research was supported by the National Natural Science Foundation of China (Project No. 81202704).

Data availability statement

Data will be made available on request.

Declaration of competing interest

The authors declare that they have no known competing financial interests or personal relationships that could have appeared to influence the work reported in this paper.

Acknowledgements

We would like to thank all the authors of this study for their exceptional cooperation as well as valuable contributions. And we thank to the Clinical Pharmacy Center, Nanfang Hospital, School of Pharmaceutical Science and School of Traditional Chinese medicine; Southern Medical University, Guangzhou, Guangdong Province, China for providing facilities for the present work.

References

[1] K. Ezzedine, V. Eleftheriadou, M. Whitton, et al., Vitiligo, Lancet 386 (9988) (2015 Jul 4) 74–84.
[2] M.L. Frisoli, K. Essien, J.E. Harris, Vitiligo: mechanisms of pathogenesis and treatment, Annu. Rev. Immunol. 38 (2020 Apr 26) 621–648.
[3] C. Bergqvist, K. Ezzedine, Vitiligo: a focus on pathogenesis and its therapeutic implications, J. Dermatol. 48 (3) (2021 Mar) 252–270.
[4] Y. Pang, S. Wu, Y. He, et al., Plant-derived compounds as promising therapeutics for vitiligo, Front. Pharmacol. 12 (2021 Nov 11), 685116.
[5] J. Ma, S. Li, L. Zhu, et al., Baicalein protects human vitiligo melanocytes from oxidative stress through activation of NF-E2-related factor2 (Nrf2) signaling pathway, Free Radic. Biol. Med. 129 (2018 Dec) 492–503.
[6] M. Hu, C. Chen, J. Liu, et al., The melanogenic effects and underlying mechanism of paeoniflorin in human melanocytes and vitiligo mice, Fitoterapia 140 (2020 Jan), 104416.
[7] Y. Deng, Z. Liu, Y. Xiao, et al., Effects of Liuweidihuang Decoction on cell proliferation and melanin synthesis of cultured human melanocytes in vitro, Nan Fang Yi Ke Da Xue Xue Bao 29 (4) (2009 Apr) 701–703.
[8] Y. Deng, L. Lv, G. Yang, et al., Role of serotoninergic/melatoninergic system in melanin metabolism in melanocytes exposed to serum of rabbits fed with Liuwei Dihuang decoction, Nan Fang Yi Ke Da Xue Xue Bao 36 (10) (2016 Oct 20) 1401–1405.
[9] Y. Deng, L. Yang, S.L. An, Effect of Tribulus terrestris L decoction of different concentrations on tyrosinase activity and the proliferation of melanocytes, Di Yi Jun Yi Da Xue Xue Bao 22 (11) (2002 Nov) 1017–1019.
[10] Z.Y. Yan, Yan Deng, Progress on the clinical mechanism of pigmented dermatosis, Hebei Traditional Chinese Medicine 38 (8) (2016) 1276–1280.
[11] Yan Deng, Zhen Liu, Yan Xiao, Effects of Liuwei Rehmannia on normal melanocyte proliferation and melanin synthesis cultured in vitro, Proceedings of Southern Medical University 29 (4) (2009) 701–703, 706.
[12] Yan Deng, X.Z. Wen, X.Z. Xiao, Effects of seroserum on tyrosinase activity, New Traditional Chinese Medicine 42 (3) (2010) 99–100.
[13] Yan Deng, L. Lv, Guang Yang, et al., Role of the serotonin/melatonin inergic system in regulating melanin metabolism in vitro, Proceedings of Southern Medical University 36 (10) (2016) 1401–1405.
[14] Y. Li, J. Yao, C. Han, et al., Quercetin, inflammation and immunity, Nutrients 8 (3) (2016 Mar 15) 167.
[15] J. Tang, P. Diao, X. Shu, et al., Quercetin and quercitrin attenuates the inflammatory response and oxidative stress in LPS-induced RAW264.7 cells: in vitro assessment and a theoretical model, Biomed Res Int. 2019 Oct 28 (2019), 7039802.
[16] M. Güran, G. Şanlıtürk, N.R. Kerküklü, et al., Combined effects of quercetin and curcumin on anti-inflammatory and antimicrobial parameters in vitro, Eur. J. Pharmacol. 859 (2019 Sep 15), 172486.
[17] K.P. Devi, D.S. Malar, S.F. Nabavi, et al., Kaempferol and inflammation: from chemistry to medicine, Pharmacol. Res. 99 (2015 Sep) 1–10.
[18] P. Rajendran, T. Rengarajan, N. Nandakumar, et al., Kaempferol, a potential cytostatic and cure for inflammatory disorders, Eur. J. Med. Chem. 86 (2014 Oct 30) 103–112.
[19] G. Iannella, A. Greco, D. Didona, et al., Vitiligo: pathogenesis, clinical variants and treatment approaches, Autoimmun. Rev. 15 (4) (2016 Apr) 335–343.
[20] A. Alikhan, L.M. Felsten, M. Daly, et al., Vitiligo: a comprehensive overview Part I. Introduction, epidemiology, quality of life, diagnosis, differential diagnosis, associations, histopathology, etiology, and work-up, J. Am. Acad. Dermatol. 65 (3) (2011 Sep) 473–491.
[21] X. Liang, H. Li, S. Li, A novel network pharmacology approach to analyse traditional herbal formulae: the Liu-Wei-Di-Huang pill as a case study, Mol. Biosyst. 10 (5) (2014 May) 1014–1022.
[22] S. Li, B. Zhang, Traditional Chinese medicine network pharmacology: theory, methodology and application, Chin. J. Nat. Med. 11 (2) (2013 Mar) 110–120.
[23] H. Xie, F. Zhou, L. Liu, et al., Vitiligo: how do oxidative stress-induced autoantigens trigger autoimmunity? J. Dermatol. Sci. 81 (1) (2016 Jan) 3–9.
[24] R. Takeyama, S. Takekoshi, H. Nagata, et al., Quercetin-induced melanogenesis in a reconstituted three-dimensional human epidermal model, J. Mol. Histol. 35 (2) (2004 Feb) 157–165.
[25] K. Yamauchi, T. Mitsunaga, M. Inagaki, et al., Quercetin derivatives regulate melanosome transportation via EPI64 inhibition and elongate the cell shape of B16 melanoma cells, Biomed. Pharmacother. 70 (2015 Mar) 206–212.
[26] Y.M. Yang, Y.O. Son, S.A. Lee, et al., Quercetin inhibits α-MSH-stimulated melanogenesis in B16F10 melanoma cells, Phytother Res. 25 (8) (2011 Aug) 1166–1173.
[27] M.M. Salem, M. Shalbaf, N.C. Gibbons, et al., Enhanced DNA binding capacity on up-regulated epidermal wild-type p53 in vitiligo by H2O2-mediated oxidation: a possible repair mechanism for DNA damage, Faseb. J. 23 (11) (2009 Nov) 3790–3807.
[28] A.T. Ha, L. Rahmawati, L. You, et al., Anti-inflammatory, antioxidant, moisturizing, and antimelanogenesis effects of quercetin 3-O-β-D-Glucuronide in human keratinocytes and melanoma cells via activation of NF-κB and AP-1 pathways, Int. J. Mol. Sci. 23 (1) (2021 Dec 31) 433.
[29] H. Tang, L. Yang, L. Wu, et al., Kaempferol, the melanogenic component of Sanguisorba officinalis, enhances dendricity and melanosome maturation/transport in melanocytes, J. Pharmacol. Sci. 147 (4) (2021 Dec) 348–357.
[30] L. Giovannelli, S. Bellandi, V. Pitozzi, et al., Increased oxidative DNA damage in mononuclear leukocytes in vitiligo, Mutat. Res. 556 (1–2) (2004 Nov 22) 101–106.
[31] Y. Wang, S. Li, C. Li, Perspectives of new advances in the pathogenesis of vitiligo: from oxidative stress to autoimmunity, Med. Sci. Mon. Int. Med. J. Exp. Clin. Res. 25 (2019 Feb 6) 1017–1023.
[32] S. Mitra, S. De Sarkar, A. Pradhan, et al., Levels of oxidative damage and proinflammatory cytokines are enhanced in patients with active vitiligo, Free Radic. Res. 51 (11–12) (2017 Dec) 986–994.
[33] S. Li, G. Zhu, Y. Yang, et al., Oxidative stress drives CD8+T-cell skin trafficking in patients with vitiligo through CXCL16 upregulation by activating the unfolded protein response in keratinocytes, J. Allergy Clin. Immunol. 140 (1) (2017 Jul) 177–189.e9.
[34] S. Li, G. Zhu, Y. Yang, et al., Oxidative stress-induced chemokine production mediates CD8(+) T cell skin trafficking in vitiligo, J. Invest. Dermatol. Symp. Proc. 17 (1) (2015 Jul) 32–33.
[35] T. Cui, W. Zhang, S. Li, et al., Oxidative stress-induced HMGB1 release from melanocytes: a paracrine mechanism underlying the cutaneous inflammation in vitiligo, J. Invest. Dermatol. 139 (10) (2019 Oct) 2174–2184.e4.
[36] K.U. Schallreuter, G. Chiuchiarelli, E. Cemeli, , et al.J.D. Spencer, H. Rokos, A. Panske, B. Chavan, J.M. Wood, D. Anderson, Estrogens can contribute to hydrogen peroxide generation and quinone-mediated DNA damage in peripheral blood lymphocytes from patients with vitiligo, J. Invest. Dermatol. 126 (5) (2006 May) 1036–1042.
[37] S. Hu, J. Huang, S. Pei, et al., Ganoderma lucidum polysaccharide inhibits UVB-induced melanogenesis by antagonizing cAMP/PKA and ROS/MAPK signaling pathways, J. Cell. Physiol. 234 (5) (2019 May) 7330–7340.
[38] L. Tang, J. Li, W. Fu, et al., Suppression of FADS1 induces ROS generation, cell cycle arrest, and apoptosis in melanocytes: implications for vitiligo, Aging (Albany NY)[J] 11 (24) (2019 Dec 21) 11829–11843.
[39] L. Wang, X. Ding, H. Huang, et al., PINK1 in normal human melanocytes: first identification and its effects on H2 O2 -induced oxidative damage, Clin. Exp. Dermatol. 46 (2) (2021 Mar) 292–299.
[40] H. Ma, X. Wang, W. Zhang, et al., Melatonin suppresses ferroptosis induced by high glucose via activation of the Nrf2/HO-1 signaling pathway in type 2 diabetic osteoporosis, Oxid. Med. Cell. Longev. (2020 Dec 4), 9067610, 2020.
[41] H. Ma, X. Wang, W. Zhang, et al., Melatonin suppresses ferroptosis induced by high glucose via activation of the Nrf2/HO-1 signaling pathway in type 2 diabetic osteoporosis, Oxid. Med. Cell. Longev. (2020 Dec 4), 9067610, 2020.
[42] Y. Li, J. Huang, J. Lu, et al., The role and mechanism of Asian medicinal plants in treating skin pigmentary disorders, J. Ethnopharmacol. 245 (2019 Dec 5), 112173.